Optimal frequency separation of power sources by multivariable LPV/Hinf control: application to on-board energy management systems of electric vehicles

Waleed Nwesaty, Antoneta Iuliana Bratcu, Olivier Sename

Optimal frequency separation of power sources by multivariable LPV/H_∞ control: application to on-board energy management systems of electric vehicles

Waleed Nwesaty, Antoneta Iuliana Bratcu, Olivier Sename

***Abstract*— In this paper a multi-variable LPV/H_∞ control approach is applied to design a strategy for power source coordination within a multi-source energy system. Three different kinds of power sources – fuel cell, battery and ultracapacitor – compose the power supply system of an electric vehicle. All sources are current-controlled and paralleled together with their associated DC-DC converters on a common DC-link coupled to vehicle's electrical motor and its converter. DC-link voltage must be regulated in spite of load power variations representing the driving cycle image. To this end, a MIMO LPV/H_∞ provides the three current references so that each source operates in its most suitable frequency range as either high-energy-density or high-power-density source: low-frequency, mean power is provided by fuel cell, ultracapacitor supplies/absorbs the instantaneous variations of power demand and battery operates in between the two other sources. Selection of H_∞ weighting functions is guided by a genetic algorithm whose optimization criterion expresses the frequency-separation requirements. The nonlinear multi-source system is simulated in MATLAB® /Simulink® using the driving cycle of IFSTTAR (Institut Français des Sciences et Technologies des Transports, de l'Aménagement et des Réseaux) as load profile, whose frequency content is richer than that of Normalized European Driving Cycle (NEDC). Simulation results show good performance in supplying the load at constant DC-link voltage according to user-configured frequency-separation power sharing strategy.**

Keywords: H_∞ control, LPV systems, power source coordination, frequency separation, electric vehicle.

I. INTRODUCTION

Modern society is facing nowadays various challenges in supplying power in response to a continuously increasing demand. This challenge is doubled by environmental requirements. In this context, a great research effort is today oriented to develop efficient and environmental friendly transportation systems [1]. In particular, car manufacturers are developing vehicles equipped with clean power sources such as fuel cells or photovoltaic panels, embedded into on-board energy management systems that ensure energy consumption minimization [2]. Auxiliary power sources like batteries and ultracapacitors can be added in order to increase efficiency by also harvesting the braking power [3]. The coordination of different sources within such embedded energy systems must then take into account the most suitable operation conditions of each source [4]. For instance, the battery state of health depends on the dynamic of its current and on the charging/discharging cycle. One can note that each source has a dynamic specialization; therefore, it should ideally operate within some given frequency range of variation. Indeed, power sources can be classified with respect to their power supply ability into two main classes [5]: high-power-density sources (able to provide high power for a short period of time with high dynamic characteristics) and high-energy-density sources (able to provide power during long period of time with slow dynamic characteristics). Ultracapacitors are typical examples of high-power-density sources, as they can provide several kilowatts in less than a second, whereas fuel cells and batteries belong to the class of high-energy-density sources because they can provide power for several hours when the load is in steady state or when charging other auxiliary sources. Performance of different source types can be identified on the well-known Ragone's plot [6].

This paper studies the case of a three-power-source power supply system – fuel cell, battery and ultracapacitor – where

Manuscript recieved March 20 2014

Waleed Nwesaty, Antoneta Iuliana Bratcu, Olivier Sename are with Grenoble Institute of Technology, GIPSA-lab, Control Systems Department, 11 Rue des Mathématiques, Grenoble Campus BP46, F-38402, Saint-Martin d'Heres, France. {waleed.nwesaty, antoneta.bratcu, olivier.sename}@gipsa-lab.grenoble-inp.fr

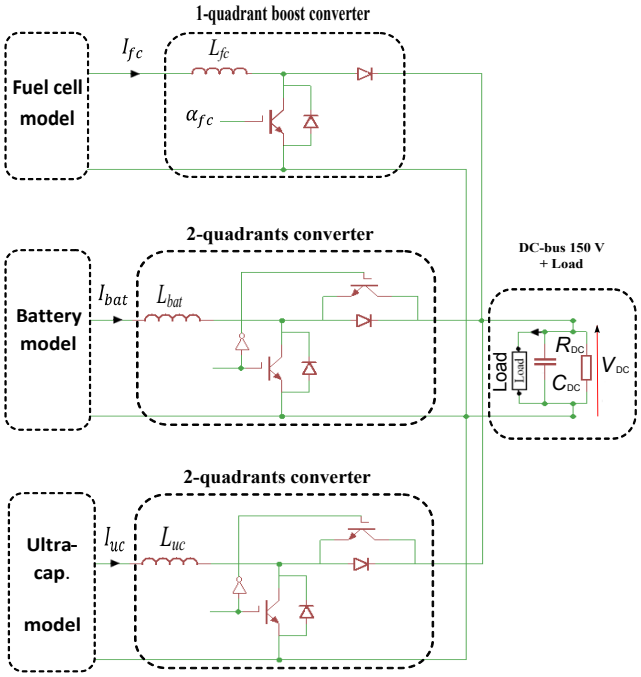

Fig. 1: System structure.

each source is controlled by means of a DC-DC converter. Sources are connected in parallel to the load (consisting of an electrical motor with its associated converter) through a DC-bus (Fig. 1). Fuel cell plays the role of the main power source, being connected to a 1-quadrant boost converter allowing only unidirectional power flow, whereas battery and ultracapacitor are used as auxiliary sources, able to respond to power demand variations placed in relatively high frequency. Each auxiliary source is connected to a 2-quadrants boost converter which allows charging/discharging.

The fuel cell is required to supply the steady-state load current (mean value), whereas power peaks and abruptly varying power variations are supplied by the ultracapacitor. The battery is well suited when power demand varies rather slowly (here, the definition of term "slow" depends on the battery type and its charging and discharging characteristics); thus, it plays a role between ultracapacitor and fuel cell. The battery can also be used to energize different equipment within the vehicle; it could play the role of the main source when the fuel cell is disconnected or empty. The system electrical scheme is presented in Fig. 1; numerical values are given in the Appendix.

The control objective of such a system is to regulate the DC-bus voltage at 150 V with a tracking error of $\pm 10\%$ in the presence of load power perturbation. To this end, a power flow coordination between sources must be achieved with respect to their frequency characteristics, which in consequence leads to improve utilization and extend life of both fuel cell and battery.

Most of works reported in the literature focus on two-power-source systems consisting, for example, of a fuel cell and a battery or an ultracapacitor as auxiliary source. In general, each source is treated as a current-controlled source, where current reference is obtained by using different methods such as PID-controller-based strategies [7], fuzzy logic control [8], or frequency-separation strategies based on high/low-pass filtering [9],[10]. LQG control has also been used to generate current references in a case of battery and ultracapacitor systems [11].

The authors have already considered in [12],[13] such a three power-source system, but implementing a different control structure. Indeed for each source, a current reference is generated by a cascade control: a PI-controller-based outer loop regulates source state of charge (SOC) with a slow dynamics and provides the low-frequency component of current reference to the PI-controller-based inner current tracking loop (fast-dynamics). For the fuel cell it is the DC-bus voltage control loop that plays the role of outer loop and , as main source, must not have high-frequency variations. For each auxiliary source, high-frequency components of current reference result from an H_∞ controller as in [12], while in [13] an LPV/H_∞ control approach is developed to handle just the variation of the operation conditions.

Different from these approaches, this paper enhances those previous studies avoiding PI-controller-based outer loops and developing a single multi-variable controller in an LPV/H_∞ approach that guarantees closed-loop global stability. Current control loops are preserved for safety reasons. The H_∞ weighting functions selection results from a genetic-algorithm-based optimization whose criterion expresses mathematically the user-supplied manner of frequency separation between the three sources.

This paper is organized as follows. Section II is dedicated to nonlinear system modeling. Section III presents the proposed control structure and details the control design procedure. Simulation results that validate the proposed approach are discussed in Section IV. Section V, the last, contains conclusion and future work.

II. MODELING

The electrical system described in Fig. 1 can be generally divided into three stages:

- Input stage: this stage consists of three power sources: fuel cell (main power source), battery and ultracapacitor (auxiliary sources), the sources are mentioned in ascending order according to their dynamic responses, where ultracapacitor is the fastest source modeled according to Fig. 2.

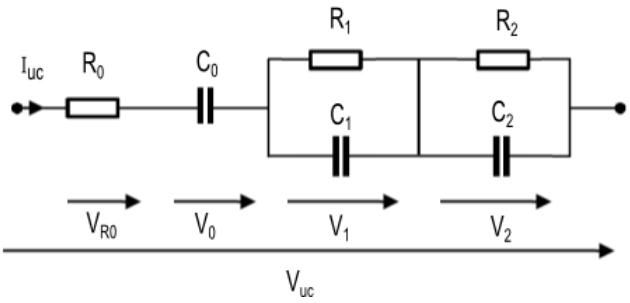

Fig. 2: Ultracapacitor electrical model.

  Fuel cell and battery are dealt with as current sources. Their models are not considered in LPV/H_∞ problem formulation (their models are used just for simulation purpose) since control objectives do not deal with their entire state dynamics. Whereas, frequency separation still required during current supply process.
- Conversion stage: each power source is connected to a DC-DC converter with respect to the source type, *i.e.*, the fuel cell is connected to 1-quadrant converter (which supplies power in one direction), whereas the other two sources are connected to 2-quadrants converters which allow bidirectional power flow and provide charging/discharging functionality to the associated source. Current closed-loop dynamics based on PI controllers are not considered in LPV//H_∞ design since they are much faster (see section III-A).
- Output stage: all previous converters are connected in parallel to DC-bus which supplies the system load. A capacitor is added to the DC-bus in order to investigate its dynamic regardless to the load type, the load could be motor with its inverter whose model is out of scope of this paper.

The energy conversion laws give the following model:

$$\begin{aligned}
\frac{dV_{dc}}{dt} &= \frac{1}{C_{DC}}[\frac{-1}{R_{DC}}V_{dc} - I_{Load} + I_{fc}(1-\alpha_{fc}) \\
&\quad + I_{bat}\alpha_{bat} + I_{uc}\alpha_{uc}] \\
\frac{dV_0}{dt} &= \frac{-1}{C_0}I_{uc} \\
\frac{dV_1}{dt} &= \frac{-1}{C_1R_1}V_1 - \frac{1}{C_1}I_{uc} \\
\frac{dV_2}{dt} &= \frac{-1}{C_2R_2}V_2 - \frac{1}{C_2}I_{uc} \\
V_{uc} &= -I_{uc}R_0 + V_0 + V_1 + V_2
\end{aligned} \tag{1}$$

where I_{fc}, I_{bat}, and I_{uc} are the currents of fuel cell, battery, and ultracapacitor respectively. $\alpha_{fc}, \alpha_{bat}$, and α_{uc} are the respective converter averaged duty cycle (averaged pulse width modulation command signals). C_{DC} and R_{DC} are the DC-bus capacitor and resistance respectively. V_{dc} is the DC-bus voltage. I_{Load} is the load current. V_{uc} is ultracapacitor voltage. R_0, C_0, R_1, C_1, R_2,and C_2 are constant parameters of ultracapacitor model. V_0, V_1 and V_2 are sub-voltages represented in ultracapacitor model (Fig. 2).

The system (1) is rewritten in the LPV form as follows:

$$\begin{cases} \dot{x} &= A.x + B_1.\omega + B_2(\rho).u \\ y &= C.x + D.u \end{cases} \tag{2}$$

where the state vector is $x = [V_{DC} \quad V_1 \quad V_2 \quad V_0]^T$. $\omega = I_{Load}$ is load current which represents the disturbance input, $u = [I_{fc} \quad I_{bat} \quad I_{uc}]^T$ is the control input vector composed of fuel cell, battery and ultracapacitor currents respectively. $\rho = [\rho_1 \quad \rho_2 \quad \rho_3]^T = [\alpha_{fc} \quad \alpha_{bat} \quad \alpha_{uc}]^T$ is the parameter vector. Matrices in (2) are:

$$A = \begin{bmatrix} \frac{-1}{C_{DC}R_{DC}} & 0 & 0 & 0 \\ 0 & \frac{-1}{C_1R_1} & 0 & 0 \\ 0 & 0 & \frac{-1}{C_2R_2} & 0 \\ 0 & 0 & 0 & 0 \end{bmatrix}$$

$$B_1 = \begin{bmatrix} \frac{-1}{C_{DC}} \\ 0 \\ 0 \\ 0 \end{bmatrix}, \qquad B_2 = \begin{bmatrix} \frac{1-\rho_1}{C_{DC}} & \frac{\rho_2}{C_{DC}} & \frac{\rho_3}{C_{DC}} \\ 0 & 0 & \frac{-1}{C_1} \\ 0 & 0 & \frac{-1}{C_2} \\ 0 & 0 & \frac{-1}{C_s} \end{bmatrix}$$

$$C = \begin{bmatrix} 1 & 0 & 0 & 0 \\ 0 & 1 & 1 & 1 \end{bmatrix}, \qquad D = \begin{bmatrix} 0 & 0 & 0 \\ 0 & 0 & -R_s \end{bmatrix}$$

The system (2) can be represented in following form:

$$\begin{bmatrix} \dot{x} \\ z \\ y \end{bmatrix} = \begin{bmatrix} A & B_1 & B_2(\rho) \\ C_1 & D_{11} & D_{12} \\ C_2 & D_{21} & D_{22} \end{bmatrix} \begin{bmatrix} x \\ \omega \\ u \end{bmatrix} \tag{3}$$

In the considered approach each parameter ρ_i is assumed to be bounded by $[0.1, 0.9]$ (this corresponds to the duty ratio accepted variation from 10% to 90%). Each parameter is supposed to be independent from the other parameters, and the system can be represented under a polytopic form with $2^3 = 8$ vertices. Note that $B_2(\rho)$ depends on the parameter vector $\rho = [\rho_1 \quad \rho_2 \quad \rho_3]^T$. This means that some filter should be used to get a simple matrix parameter-independent as in [14],[15].

III. Control design

This section details the control approach used to perform on-board power sources coordination. The control objectives are:

1) DC-bus voltage is regulated to 150V$\pm$10% regardless of the current load demand.
2) Apply frequency separation to power sources, *i.e.*, each power source supplies power with respect to its frequency characteristic. That is achieved due to the choice of weighting functions associated to H_∞ control design.
3) Regulate the state of charge of the ultracapacitor to 50% which allows to absorb/provide power to fulfill instantaneous load power demand.
4) Impose a desired steady-state behavior for the rest of the power sources, *i.e.*, fuel cell and battery.

The control loop consists mainly of two nested levels, as shown in Fig. 3:

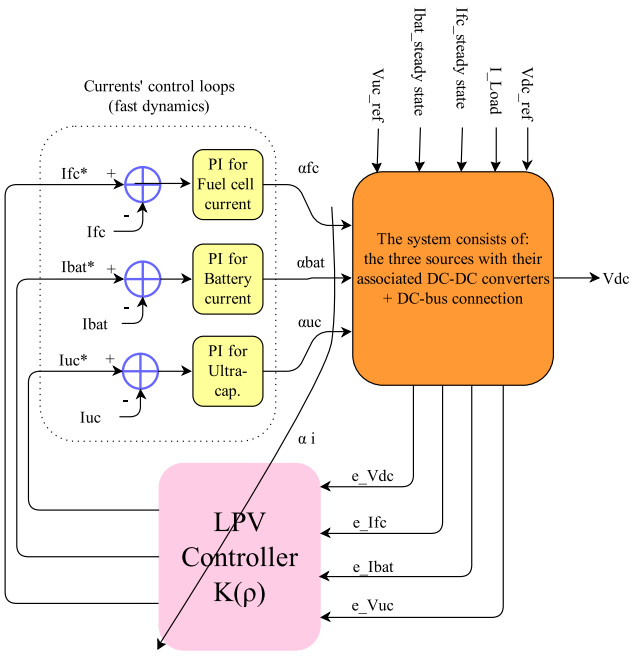

Fig. 3: Global control block diagram.

A. Current control level

According to power electronics design and application, it is preferred to control each power source current and prevent it from exceeding admissible limits. Therefore, three different PI-controllers are used to control the converters and required to ensure dynamics faster than the outer level. These control loops are transparent to the outer level and satisfy tracking of all current references generated by LPV controller (Fig. 3), therefore we will consider in the sequel $I_{fc}{}^*$=I_{fc}, $I_{bat}{}^*$=I_{bat} and $I_{uc}{}^*$=I_{uc}.

B. LPV control level

This level coordinates the system sources generating the sources' current references. To this end, an LPV/H_∞ controller is synthesized to meet the control objectives, and to emphasize the sources' frequency splitting.

1) H_∞ control problem formulation: LPV/H_∞ control is used in this context not only to ensure closed-loop system stability, but also to meet the following control objectives using weighting functions represented in the generalized form (Fig. 4):

1) Tracking of DC-bus voltage V_{DC}: this is achieved using $W_{eV_{dc}}$ which determines both time response and acceptable tracking error range.
2) Power sources frequency splitting: this is achieved thanks to W_{uIfc}, W_{uIbat} and W_{uIuc} that impose the dynamic current supply (control input vector) of the fuel cell, the battery and the ultracapacitor, respectively, according to the pre-specified frequency ranges.
3) Tracking of ultracapacitor state of charge (SOC): this is achieved using $W_{eV_{uc}}$ to maintain its voltage around 37V which corresponds to 50% SOC (the voltage is a direct image of SOC in the ultracapacitor case).
4) Impose steady state behavior for the fuel cell and the battery: this is achieved using $W_{eI_{fc}}$ and $W_{eI_{bat}}$, respectively. This is interesting for imposing a desired steady-state power sharing using $I_{fc_{steadystate}}$ and $I_{bat_{steadystate}}$ reference inputs.

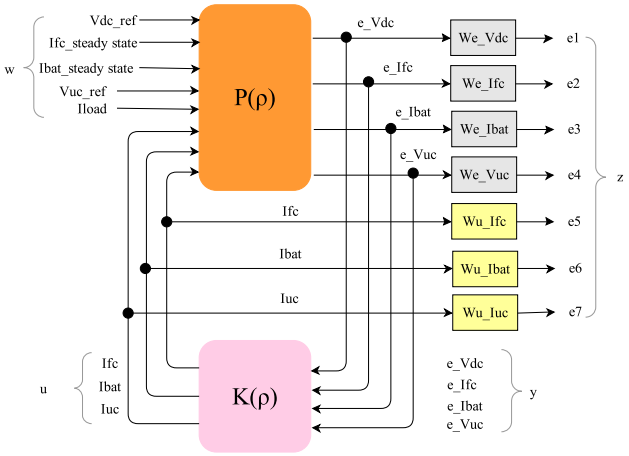

Fig. 4: H_∞ Robust control design block diagram.

Remark (about the 4^{th} control objective):

Notice that all power sources should be able to provide steady state currents (*e.g.*, fuel cell case) or drag DC current (*e.g.*, the case when charging battery or ultracapacitor). In order to include such a requirement in the H_∞ framework, two external reference inputs are added to provide DC components for battery and fuel cell currents. These two reference inputs provide some degrees of freedom in the problem formulation, besides they are useful to easily determine charging procedure for the battery depending on its type (out of scope of this work).

Fig. 4 represents the general control configuration for the LPV/H_∞ controller synthesis.

2) Weighting functions selection: To cope with the performance requirements we have chosen usual form of the weighting functions. Thus, it has been considered that:

- DC-bus voltage, ultracapacitor voltage (state of charge) and fuel cell current are bounded by first-order weighting functions $W_{eV_{dc}}, W_{eV_{uc}}$ and W_{uIfc}, respectively.
- Battery and ultracapacitor currents are bounded by fourth-order band-pass weighting function $W_{uI_{bat}}, W_{uI_{uc}}$, respectively, this fourth order choice is to ensure separation within narrow frequency interval.
- Steady-state fuel cell and battery currents are bounded by constants weighting functions $W_{eI_{fc}}$ and $W_{eI_{bat}}$, respectively.

Then 19 parameters have to be chosen in order to achieve the closed-loop performance. This selection is the key issue in the H_∞control design, and is quite a complex problem. In order to propose an efficient and repeatable way of control design, an optimization procedure based on Genetic Algorithm (GA) has been considered as proposed in [16]. Such a procedure requires objective (cost) functions to be minimized to meet the optimal performance objectives. In our case, GA is applied to minimize two objective functions:

- Objective function 1 (closed-loop stability): it is based on minimizing the maximum eigenvalue of the closed-loop system to be smaller than a certain desired degree δ.

$$f_1 = min\{\max_i(Re(\lambda_i)) < -\delta : \delta > 0\} \qquad (4)$$

  where $Re(\lambda_i)$ is the real part of the eigen value λ_i.
- Objective function 2 (frequency splitting between power source): it is based on minimizing the following criterion:

$$f_2 = min\left\{\frac{J_1 + J_2 + J_3}{3}\right\} \qquad (5)$$

  with

$$J_1 = \frac{\left\|\frac{I_{fc}}{I_{load}}\right\|_{\infty,(\omega_1,\omega_2)}}{\left\|\frac{I_{fc}}{I_{load}}\right\|_{\infty}}$$

$$J_2 = \frac{1}{2}.\frac{\left\|\frac{I_{bat}}{I_{load}}\right\|_{\infty,(\omega_3,\omega_4)}}{\left\|\frac{I_{bat}}{I_{load}}\right\|_{\infty}} + \frac{1}{2}.\frac{\left\|\frac{I_{bat}}{I_{load}}\right\|_{\infty,(\omega_5,\omega_6)}}{\left\|\frac{I_{bat}}{I_{load}}\right\|_{\infty}}$$

$$J_3 = \frac{\left\|\frac{I_{uc}}{I_{load}}\right\|_{\infty,(\omega_7,\omega_8)}}{\left\|\frac{I_{uc}}{I_{load}}\right\|_{\infty}}$$

  where $\|.\|_{\infty,(\omega_i,\omega_j)}$ is the H_∞ norm calculated within $[\omega_i, \omega_j]$ frequency interval.

The criteria (5),(6) guarantees certain degree of closed-loop stability and allow to emphasize frequency separation between power sources.

GA tries in first generation to find good parameters randomly, then it develops each generation to minimize

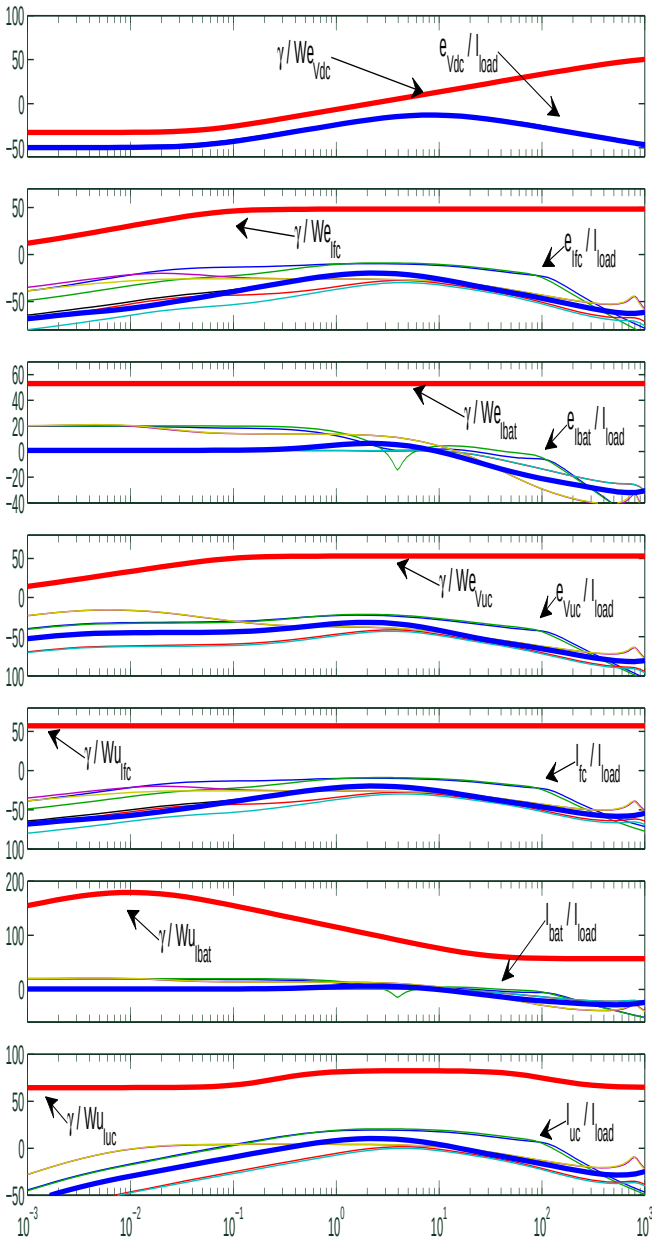

Fig. 5: Bode diagram amplitude for closed-loop transfer functions from I_{load} perturbation input to controlled outputs ($\frac{e_{Vdc}}{I_{load}}, \frac{e_{Ifc}}{I_{load}}, \frac{e_{Ibat}}{I_{load}}, \frac{e_{Vuc}}{I_{load}}, \frac{I_{fc}}{I_{load}}, \frac{I_{bat}}{I_{load}} and \frac{I_{uc}}{I_{load}} respectivily$)

with their corresponding weighting functions found by genetic algorithm.

the desired cost functions (more information about genetic algorithm can be found in [16]).

As a result, weighting functions We, Wu are obtained using GA and shown in Fig. 5.

3) LPV controller synthesis: Following the methodology in the framework of quadratic stabilization described in [17],[18], the problem solvability consists in solving a set of LMIs (using Yalmip/Sedumi solver), at each vertex of the polytop (parameter set). This allows to find the "vertex controllers": $K_i = \begin{bmatrix} A_i & B_i \\ C_i & D_i \end{bmatrix}$ .Then, the LPV controller $K(\rho)$ is a convex combination of the vertex controllers K_i as follows:

$$K(\rho) = \sum_{1}^{8} \alpha_i(\rho) K_i \tag{6}$$

with:

$$\alpha_i(\rho) = \frac{\prod_{j=1}^{3} |\rho_j - C(w_i)_j|}{\prod_{j=1}^{3} \left|\overline{\rho_j} - \underline{\rho_j})\right|} > 0 \quad \sum_{1}^{8} \alpha_i = 1$$

ω_i are the extremities of the polytope formed by the extreme values of the parameter vector ρ. $C(w_i)_j$ is the j^{th} component of the vector $C(w_i)$ defined as:

$C(w_i)_j = \{\rho_j | \rho_j = \overline{\rho_j}$ if $\omega_i = \underline{\rho_j}$ otherwise $\rho_j = \underline{\rho_j}\}$.
with

$$\overline{\rho_j} = max(\rho_j) = 0.9 \qquad \underline{\rho_j} = min(\rho_j) = 0.1$$

IV. Simulation results

Numerical simulations under MATLAB® /Simulink® show the effectiveness of the proposed LPV/H_∞ control approach. The simulations are carried out using nonlinear electrical models for different system's parts. The driving cycle proposed by IFSTTAR [11] is chosen to prove the closed loop system capability to cope with multiple driving mode and satisfy the required control objectives (Fig. 6); this driving cycle has a frequency content richer than that of Normalized European Driving Cycle (NEDC) [19]. IFSTTAR profile represents various driving conditions including acceleration, deceleration, steady speed and full brake and allow assessing performance of DC-bus voltage regulation and the way how the three sources are coordinated to provide the demanded power. For this scenario, external references for steady state inputs are: $I_{fc_{steadystate}} = \frac{I_{load}}{1-\alpha_{fc}}$ which implies that load current is served exclusively by fuel cell at steady-state. $I_{bat_{steadystate}} = 0$ means no change for SOC battery at steady-state.

Another simulation scenario is tested when the load is a constant current, this scenario illustrates how the two external inputs determine the fuel cell and battery steady-state behaviors.

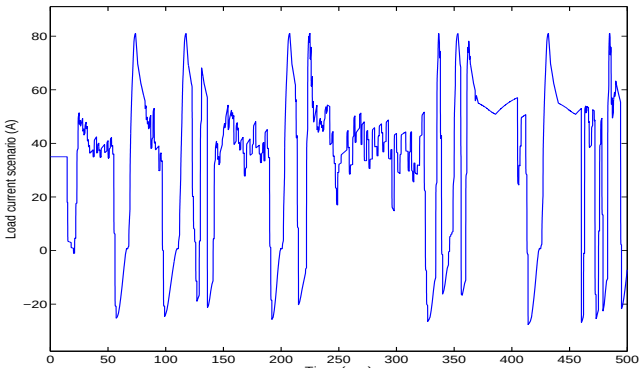

Fig. 6: IFSTTAR load current scenario used in simulation (test A).

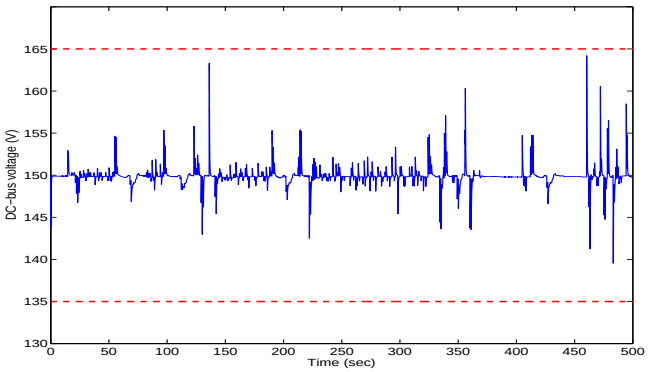

Fig. 7: DC-bus regulated voltage corresponding to IFSTTAR load scenario, voltage is well regulated to 150 V $\pm 10\%$ as an accepted error (test A).

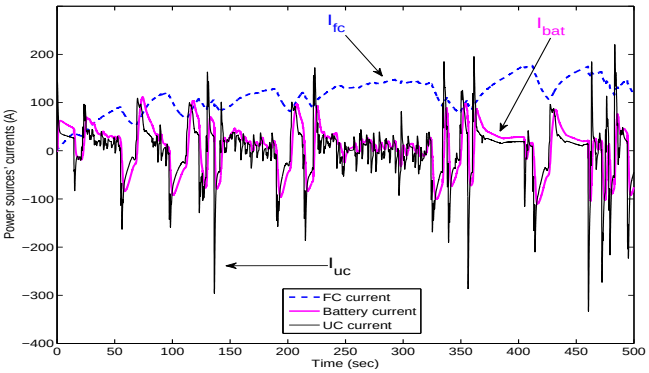

Fig. 8: Sources' currents corresponding to IFSTTAR load scenario (test A).

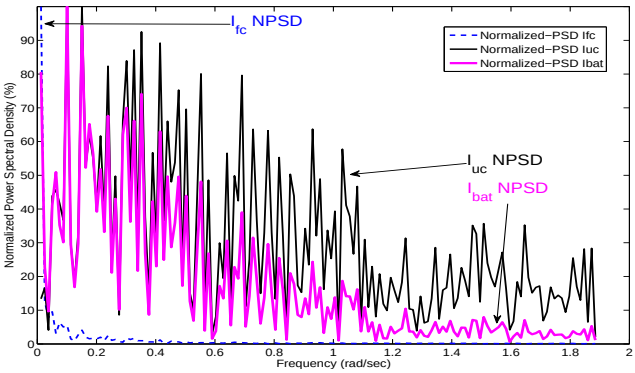

Fig. 9: Normalized power spectral density of each source's current corresponds to its maximum value, IFSTTAR load scenario (test A).

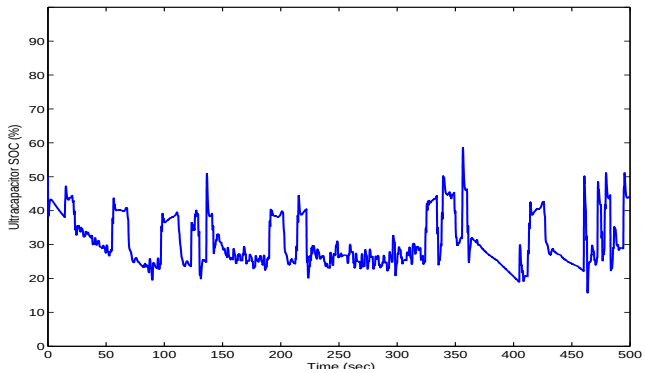

Fig. 10: Ultracapacitor state of charge variation during IFSTTAR simulation scenario (test A).

A. *IFSTTAR driving cycle test*

The goal of this test is to illustrate control objectives 1, 2 and 3 of section III. This load profile is rich in frequency content and challenges the vehicle's power supply management system in a way corresponding to urban driving conditions. The demanded power is provided by the three sources in their respective frequency ranges, while DC-bus voltage is well regulated within the accepted tracking error range.

Fig. 7 shows that DC-bus control objective is satisfied regardless of load current demand. Power sources provide currents to satisfy load demand in different frequency zones according to Fig. 8 and Fig. 9, where the last one represents the normalized power spectrum density calculated for each source current in order to show this frequency separation. Another control objective is satisfied (Fig. 10) where ultracapacitor state of charge is kept around 50%, that makes the ultracapacitor ready to provide/absorb instantaneous load current demand.

B. *Constant load test*

In order to illustrate the 4^{th} control objective (Section 4), a simple simulation scenario is given now, where the external references define the steady-state distribution of the fuel cell and the battery currents. Therefore, a constant load current (35 A) is used to allow the system to reach its steady state. Two scenarios are shown:

- $I_{fc_{steadystate}} = \frac{0.7*35}{1-\alpha_{fc_{steadystate}}} = 81A$ and $I_{batsteadystate} = \frac{0.3*35}{\alpha_{batsteadystate}} = 30A$: this corresponds to $70\% I_{load}$ is supplied by the fuel cell and 30% by the battery.
- $I_{fc_{steadystate}} = \frac{1.3*35}{1-\alpha_{fc_{steadystate}}} = 190A$ and $I_{batsteadystate} = \frac{-0.3*35}{\alpha_{batsteadystate}} = -24.5A$: this corresponds to 130% I_{load} is supplied by the fuel cell and -30% by the battery, meaning that the fuel cell is managed to supply load current and to charge the battery at the same time.

Fig. 11 and Fig. 12 show the slow dynamics imposed for the control inputs I_{fc} and I_{bat} corresponding to different constant current demand. From an application point of view, these two external inputs are helpful to impose a desired steady-state operating point which can serve charging process for the battery.

Note that there exists a slight tracking error in tracking objective, this could be handled with more complex weighting functions $W_{eI_{fc}}$ and $W_{eI_{bat}}$.

V. CONCLUSIONS AND FUTURE WORKS

A. *Conclusions*

In this paper, a multi-variable LPV/H_∞ control approach is applied to design a strategy for a multi-source energy system coordination. The studied system is based on three

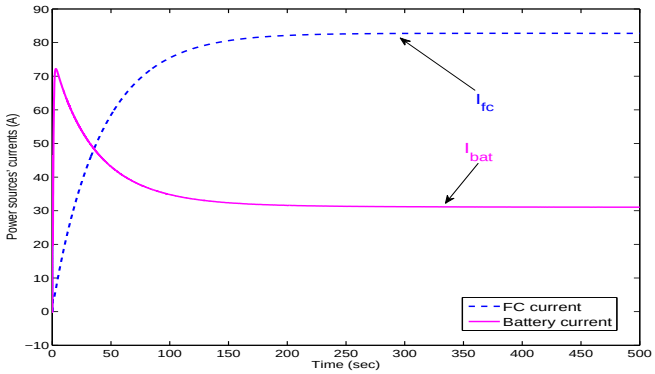

Fig. 11: Steady-state behavior for constant load scenario (test B), where 70% and 30% of I_{load} is supplied by the fuel cell and the battery, respectively.

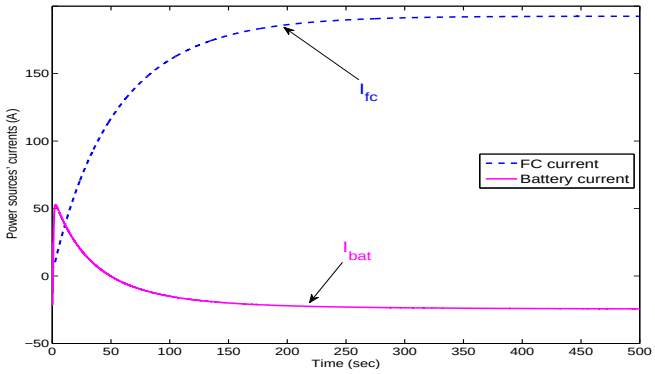

Fig. 12: Steady-state behavior for constant load scenario (test B), where fuel cell supplies 100% of I_{load} and charge the battery at the same time.

different kinds of power sources – fuel cell, battery and ultracapacitor – on board of an electric vehicle. Current-controlled sources are connected in parallel with their associated DC-DC boost converters on a common DC-bus and coupled to the load (an electrical motor with its converter). The DC-bus voltage is regulated in spite of load power variations that represent the image of driving cycle. Fuel cell and battery are protected from sudden power variations to preserve their states of health, therefore each source should be operated in the frequency range that suits best its features as either high-energy-density or high-power-density source, according to Ragone's taxonomy. Thus, fuel cell is managed to provide the low-frequency, mean power, ultracapacitor provides/absorbs the sudden variations of power demand and battery operation is placed in between the two other sources. Frequency-separation requirements are cast into an optimization criterion used to guide computation of H_∞ weighting functions by means of a genetic algorithm. LPV control approach guarantees the existence of a single Lyapunov function for all operating points and allows to design an unique controller, which greatly simplifies the implementation.

The nonlinear electrical system is simulated using the driving cycle of IFSTTAR institute as load profile, whose frequency content is richer than that of Normalized European Driving Cycle (NEDC). Numerical simulation results show good performance in supplying the load according to the frequency-separation power sharing strategy imposed by user, all by regulating the DC-bus voltage at the desired setpoint.

B. Future Works

Future work can concern the extension of system operating regimes by varying the use of different sources (*e.g.*, fuel cell could be required only to recharge the other sources at its maximum efficiency working point). Generalization of the proposed power sharing control strategy to any kind of on-board energy management systems, potentially containing any number of power sources, could be considered. Experimental validation on a dedicated test bench is envisaged in the very next future.

APPENDIX

Ultracapacitor converter: L_{uc}=0.5 mH; PI-controller: K_p = 10.10^{-3}, K_i =0.4. Battery converter: L_{bat}=0.5 mH; PI-controller: K_p = 10.10^{-3}, K_i =0.8. Fuel cell converter: L_{fc}=6 mH; PI-controller: K_p = 0.5, K_i =0.1. DC-bus: V_{DC}=150 V, C_{DC}=22 mF, R_{DC}=100 kΩ.

REFERENCES

[1] H. Rahimi-Eichi, U. Ojha, F. Baronti, and M.-Y. Chow, "Battery Management System – An Overview of Its Application in the Smart Grid and Electric Vehicles", *IEEE Industrial Electronics Magazine*, vol. 7, no. 2, 2013, pp. 4-16.

[2] C. Li, G. Liu, "Optimal fuzzy power control and management of fuel cell/battery hybrid vehicles", *Power Sources J.*, vol.192, 2009, pp. 525-533.

[3] E. Ozatay, B. Zile, J. Anstrom , S. Brennan, "Power Distribution Control Coordinating Ultracapacitors and Batteries for Electric Vehicles," *Proceedings of the 2004 American Control Conference Boston, Massachusetts*, USA, 2004, pp. 4716-4721.

[4] D. Iannuzzi, "Use of Supercapacitors, Fuel cells and Electrochemical Batteries for Electric Road Vehicles: A Control Strategy," *The 33rd Annual Conference of the IEEE Industrial Electronics Society (IECON) Nov. 5-8*, Taipei, Taiwan, 2007, pp. 539-544.

[5] P. Thounthonga, S. Raël, B. Davat, "Energy management of fuel cell/battery/supercapacitor hybrid power source for vehicle applications," *Power Sources J.*, vol.193, 2009, pp. 376-385.

[6] A. Kuperman, I. Aharon, "Battery–ultracapacitor hybrids for pulsed current loads," *Renewable and Sustainable Energy Reviews 15*, 2011, pp. 981-992.

[7] J. Wong, N.R.N. Idris, M. Anwari, T. Taufik, "A Parallel Energy-Sharing Control for Fuel cell-Battery-Ultracapacitor Hybrid Vehicle", *Proceedings of Energy Conversion Congress and Exposition (ECCE) IEEE,* , 2011, pp. 2923- 2929.

[8] A. Fadel, B. Zhou, "An experimental and analytical comparison study of power management methodologies of fuel cell–battery hybrid vehicles", *Power Sources J.*, vol.196, 2011, pp. 3271-3279.

[9] A. Florescu, I. Munteanu, A.I. Bratcu and S. Bacha, "Frequency-Sepation-Based Energy management Control Strategy of Power Flows within Electric Vehicles using Ultracapacitors", *IECON2012 (38th Annual Conference of the IEEE Industrial Electronics Society)*, Montréal, Canada, 2012.

[10] A. Florescu, I. Munteanu, A.I. Bratcu, A. Rumeau and S. Bacha, "Results Concerning Ultracapacitor-based Energy Management Strategy within Electric Vehicles", *ICSTCC2012 (16th International Conference on System Theory, Control and Computing)*, Sinaia, Romania, 2012.

[11] A. Florescu, A.I. Bratcu, I. Munteanu and S. Bacha, "Energy Management System within Electric Vehicles Using Ultracacitors : An LQG-optimal-control-based Solution", *CAO'2012 (15th IFAC Workshop on Control Applications of Optimization)*, Rimini, Italy, 2012.

[12] W. Nwesaty, A. I. Bratcu and O. Sename "MIMO H_∞ control for power source coordination – application to energy management systems of electric vehicles," *Accepted at* 19^th *IFAC World Congress*, 2014.

[13] W. Nwesaty, A. I. Bratcu and O. Sename "LPV control for power source coordination. application to electric vehicles energy management systems," *Accepted at European Control Conference (ECC)*, 2014.

[14] C.W. Scherer, "Mixed H_2/H_∞ control for time-varying and linear parametrically-varying systems", *Int. J. of Robust and Nonlinear Control 9-10*, 1996, pp 929-952

[15] C. Poussot-Vassal, "Multi-variables LPV robust control for vehicle chasis", *Phd thesis. Grenoble INP*, Grenoble, France, 2008.

[16] D. Goldberg, "Genetic Algorithms in Searching Optimisation and Machine Learning", *Addison-Wesley Longman*, 1989.

[17] P. Apkarian, P. Gahinet and G. Becker, "Self-scheduled Hinf Control of linear parameter-varying system: a design example", *Automatica*, vol. 31, No. 9, 1995, PP. 1251-1261.

[18] A.L. Do and O. Sename and L. Dugard, LPV modelling and control of semi-active dampers in automotive systems, Chapter 15 in *Control of Linear Parameter Varying Systems with Applications*, *Springer, J.Mohammadpour and C. Scherer (Eds)*, 2012.

[19] T. J. Barlow, S. Lathman, I. S. McCrae and P. G. Boulter, "A reference book of driving cycles for use in the measurement of the road vehicle emissions", *Technical Report PPR354*, $www.gov.uk/government/uploads/system/uploads/attachment_data/file/4247/ppr-354.pdf$, *(available March 2014)*.